LCLS-II Technical Note

Transverse Wakefields and Alignment of the LCLS-II Kicker and Septum Magnets

LCLS-II TN-16-13

12/12/2016

P. Emma, J. Amann,K. Bane,
Y. Nosochkov, M. Woodley

1 Introduction

The LCLS-II includes several fast kicker magnets, with ceramic vacuum chambers and thin conductive coating, and DC Lambertson septum magnets, all of which need special alignment attention in order to provide the necessary beam stay-clear in their small apertures, and also to limit transverse (*i.e.*, vertical) resistive-wall wakefield effects, as the beam typically passes off-axis in some of these magnets. The kicker magnets addressed here are: 1) the diagnostic kicker at 100 MeV, 2) the HXR spreader kicker at 4 GeV, and 3) the SXR spreader kicker at 4 GeV. Each of these kickers (when triggered) deflect the beam vertically (up), with the slight complication that the diagnostic kicker (DIAG0) is rolled by 10 degrees around the beam direction axis. Each kicker is followed by a septum magnet to convert the small vertical kick (a 15-mm vertical beam displacement at the septum face for each kicker) into a large horizontal bend. (Note that the DIAG0 septum is also rolled by 10 degrees.) The kicker magnet parameters are listed in Table 1 and the septum magnet parameters are in Table 2. Note that the spreader kickers are actually composed of three 1-m long magnets with 30-cm spacing gaps, but we ignore this detail here and treat these kickers as 3-m long magnets. Note that the kicker vacuum chambers also generate a longitudinal resistive-wall wakefield which generates a small energy chirp at the level of 0.01%, but the longitudinal wake is independent of transverse alignment, so it is not discussed here.

A final summary section at the end of this document prescribes all of the misalignments that should be applied to each magnet, and its associated vacuum chamber, in order to maximize the beam stay-clear and minimize transverse wakefields.

Table 1: The three LCLS-II **kicker magnets** and their nominal parameters.

Parameter	**Symbol**	**DIAG0**	**HXR**	**SXR**	**units**
Electron energy	E	0.1	4	4	GeV
Magnet bore ID (cylindrical)	$2r$	25	10	10	mm
x/y beta function (at kicker center)	$\beta_{x,y}$	13/16	94/55	56/56	m/m
Roll angle (around beam direction)	ϕ	10	0	0	deg
Nom. bend angle (~ up)	θ	8.33[1]	0.75	0.75	mrad
Vertical beam displacement at septum face	-	15	15	15	mm
Net kicker magnet length	L	1	3	3	m
Nom. magnetic field when triggered	$\lvert B_x \rvert$	0.0278	0.0334	0.0334	kG
Maximum trigger rate	-	120	10^6	10^6	Hz

[1] This bend angle is measured along the 10-deg rolled transverse coordinates.

Table 2: The three LCLS-II **septum magnets** and their nominal parameters. The electron energy at each septum is the same as its adjacent kicker.

Parameter	Symbol	DIAG0	HXR	SXR	units
Field-free region bore (cylindrical ID)	$2r$	20	20	20	mm
Field-region (rectangular full gap height)	-	16.5	14.5	14.5	mm
x/y beta function (at magnet center)	$\beta_{x,y}$	0.6/6	22/36	58/19	m/m
Roll angle (around beam direction)	ϕ	10	0	0	deg
Nom. bend angle (horizontal)	-	105	5.53	–11.1	mrad
Nom. magnetic field	$\lvert B_y \rvert$	0.88	0.74	1.48	kG
Septum magnet length	L	0.4	1	1	m

The electron beam can be quickly switched into any of four destinations by triggering the appropriate kicker to optionally send beam to the diagnostic line, the HXR FEL, the SXR FEL, or the BSY dump. The three kicker locations are indicated in Figure 1 with yellow circles.

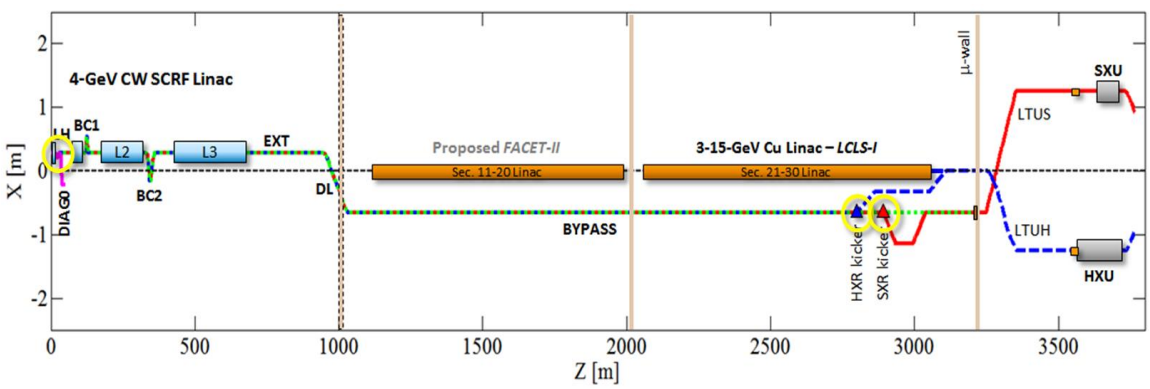

Figure 1: The locations (yellow circles) of the three kicker magnets along the LCLS-II accelerator.

2 Transverse Wakefields

Since the beam is kicked vertically, the electron bunch will travel off axis in the vacuum chamber of each kicker, generating a transverse resistive-wall wakefield which depends on the mean vertical beam offset, $\langle y \rangle$, the bunch charge, Q, the electron energy, E, the kicker aperture radius, r, the FWHM bunch length, Δs, the kicker length, L, and the resistivity, ρ, of the metallic coating inside the ceramic vacuum chamber. An exaggerated kicker trajectory is shown in Figure 2. If the net kick angle is described as $\theta (<< 1)$, and the kicker length is L, this generates an average vertical beam offset in the chamber of $\langle y \rangle = \theta L/6$, which linearly scales the wakefield kick (ignoring the detailed trajectory curvature).

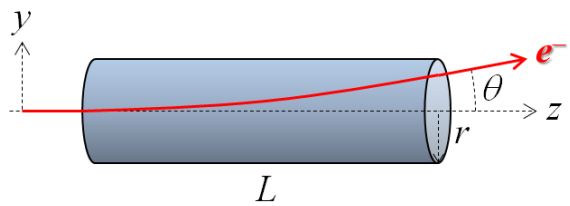

Figure 2: An exaggerated electron trajectory (red) arcing through the cylindrical vacuum chamber of a kicker (when triggered). The net kick angle is θ, the kicker length is L, and the average vertical offset, integrated over L, is $\langle y \rangle = \theta L/6$. The inner pipe radius is r.

Note that the un-kicked trajectory is nominally centered in the pipe when the kicker is not triggered, so both possible trajectories should be considered when proposing an alignment strategy to minimize wakefields. A vertical alignment bias of the magnet/chamber may reduce the wakes for one trajectory, but increase the wakes for the other.

Figure 3 shows the transverse normalized wakefield (for the spreader kicker) along the bunch length coordinate, s, for an average offset of $\langle y \rangle = \theta L/6 = 0.375$ mm, for a 100-pC case and a 300-pC case. Note that the wakefield kick is normalized here to the rms vertical beam divergence at that location, $\sigma_y' \equiv (\varepsilon_y/\beta_y)^{1/2}$, where the emittance is $\gamma\varepsilon_y = 0.5$ μm, and the kicker beta functions, β_y, are listed in Table 1. The peak normalized wakefield kick at the tail of the bunch (at right) needs to be small, $|\Delta y'|/\sigma_y' << 1$, for best FEL performance.

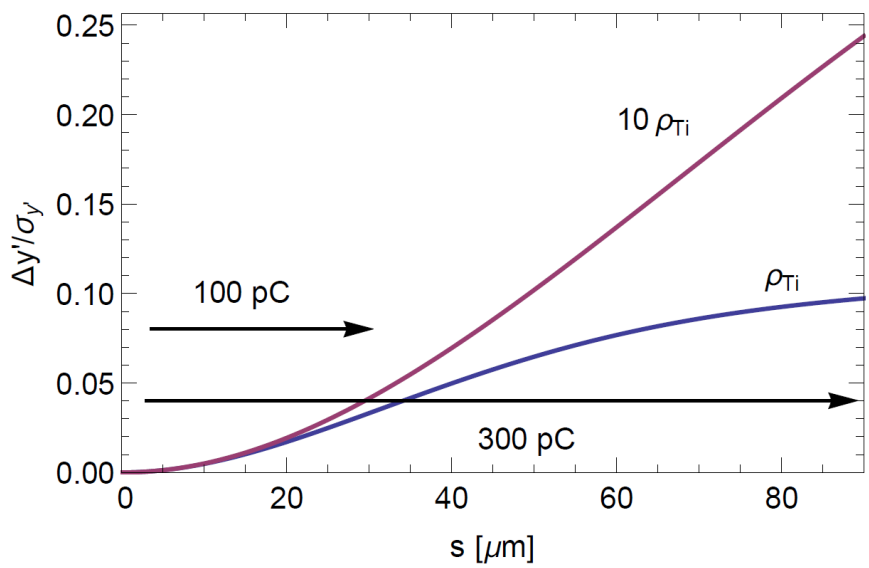

Figure 3: Transverse normalized wake (spreader kicker) along bunch length coordinate, s, for 100 and 300 pC, and 0.375-mm mean vertical position, $\langle y \rangle$. The temporal distribution is uniform with 30-μm FWHM bunch length at 100 pC (short arrow) or 90 μm at 300 pC (long arrow), for 1-kA peak current in each case. The resistivity of Ti (blue) is 43 μOhm-cm, while the resistivity for TiN (purple) is taken 10-times larger than Ti.

The plot shows the wakes for the electrical resistivity of Ti (43 μOhm-cm), and also for 10-times the resistivity of Ti as a conservative estimate for the thin TiN coating. The temporal distribution is uniform here with a 30-μm FWHM bunch length at 100 pC (extent of short arrow)

or 90 μm at 300 pC (extent of long arrow), for a 1-kA peak current in each case. For this conservative TiN coating resistivity, the normalized peak (at tail) wake-kick is 0.24 for the 300-pC case, or 0.04 for the 100-pC case. This is small but can be reduced further with magnet alignment adjustments, as described below. The table below lists these results, and the peak calculated normalized wakefield kick for each of the three kickers, where no intentional magnet misalignment compensation is applied yet.

Table 3: The three kicker magnets and their wakefield parameters (no misalignments applied yet).

Parameter	symbol	DIAG0	HXR	SXR	units
Kicker chamber bore radius	r	12.5	5	5	mm
Bunch charge (max.)	Q	300	300	300	pC
Bunch length (FWHM, uniform)	Δs	5.0	0.09	0.09	mm
Chamber coating (TiN) resistivity*	ρ	430	430	430	μOhm-cm
Average vertical trajectory in kicker	$\langle y \rangle$	1.4	0.4	0.4	mm
Calculated norm. wakefield kick	$\Delta y'/\sigma_y'$	0.01	0.24	0.24	-

* The resistivity of TiN was conservatively estimated by using 10-times that of Ti (at 30 °C).

Note that the vertical betatron phase advance, $\Delta\psi_y$, between the two spreader kickers is 100°, so optical cancelation schemes are not easily arranged. It is difficult to adjust this phase advance closer to 180 degrees since the vertical beta function at each kicker is constrained to $\beta_y < 60$ m in order to reduce the effects of kicker amplitude jitter on the FEL stability.

The septum magnets have much smaller wakefields since these are DC magnets and do not require TiN-coated chambers. The transverse wakefields for the septum magnets, including intentional magnet misalignments as described below, are very small and summarized near the end in Figure 13.

3 Diagnostic Kicker and Septum

The low-energy diagnostic kicker is described in Table 1 and Table 3, and the diagnostic septum magnet cross-section is shown in Figure 4, with a 20-mm ID field-free region and a 16.5-mm full vertical gap between the poles (beam exits out of the paper throughout). The iron bridge separating the field-region from the field-free region is 3 mm thick at its narrowest.

The diagnostic kicker has a larger bore and a shorter length than the spreader kickers, but a lower beam energy and longer bunch. Assuming the same TiN chamber coating, a 1.4-mm average vertical position along the kicker (for the kicked beam only), a 5-mm FWHM bunch length at 300 pC, and the wakefield parameters listed in Table 3, the normalized peak wakefield kick (for the kicked beam) is $\Delta y'/\sigma_y' \approx 0.01$, if no intentional alignment bias is added. This is very small and equivalent to < 0.01% relative y-emittance growth ($\Delta\varepsilon_y/\varepsilon_y \approx 0.5[\Delta y'/\sigma_y']^2$).

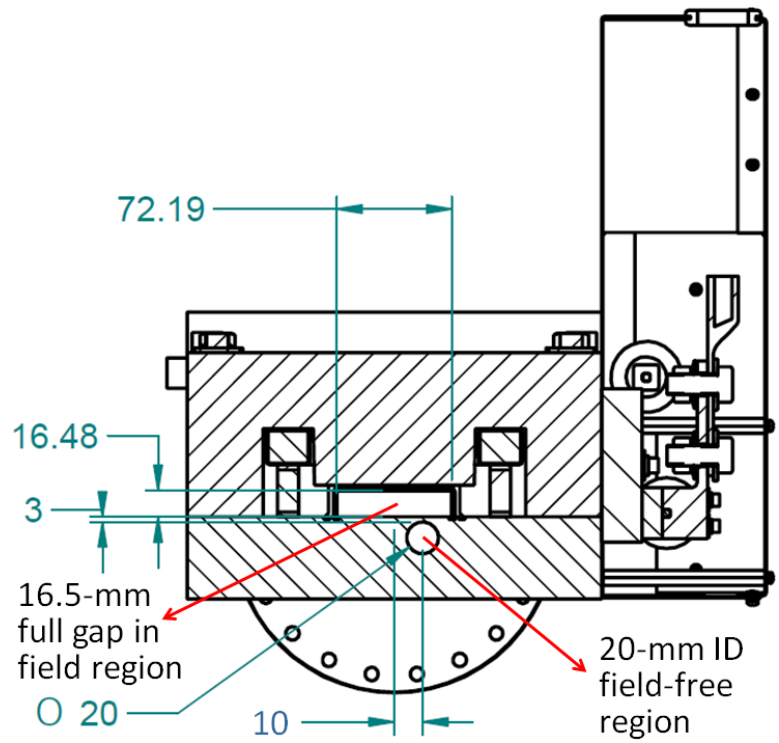

Figure 4: Cross-section (beam out of the paper) of **diagnostic** septum magnet with 20-mm cylindrical ID in the field-free region, and a 16.5-mm full vertical gap in the rectangular field-region. The iron bridge separating the field-region from the field-free region is 3 mm at its narrowest. All dimensions in the figure are in mm. The field-free cylindrical bore is biased horizontally by 10 mm (to the right here) with respect to the pole centers.

Since the un-kicked beam has no average offset in the kicker, unless we add one, there is no transverse wakefield there. And since the un-kicked beam drives the FEL, and is therefore the most important in terms of preserving beam brightness, we choose to add no intentional kicker/chamber offset here. The very small wake on the diagnostic kicker is acceptable without alignment compensation, and likely unmeasurable in any case.

The diagnostic kicker cross-section is shown in Figure 5 (beam directed toward reader) and depicts the magnet vacuum chamber, the beam stay-clear, and the ±6-sigma beam sizes, each shown before and after the kicker. In addition, the diagnostic septum cross-section is shown in Figure 6 with a 10-deg rolled magnet and bore dimensions as described in the caption.

Finally, note that the beam makes a large horizontal sweep from start to end of the septum magnet, as shown in Figure 6. The beam slides about 21 mm horizontally as it arcs through the septum chamber. To keep the beam roughly centered horizontally in the magnetic poles, the cylindrical aperture is biased horizontally, with respect to the center of the rectangular aperture, by 10 mm, making the beam less sensitive to field roll-off effects near the magnetic pole edges. Note this horizontal offset is not necessary for the spreader septum magnets (see Figure 10 and Figure 12) since the beam arc sweeps by < 3 mm in HXR, and < 6 mm in SXR. The two spreader septa magnets are then identical in design, although different in field excitation level.

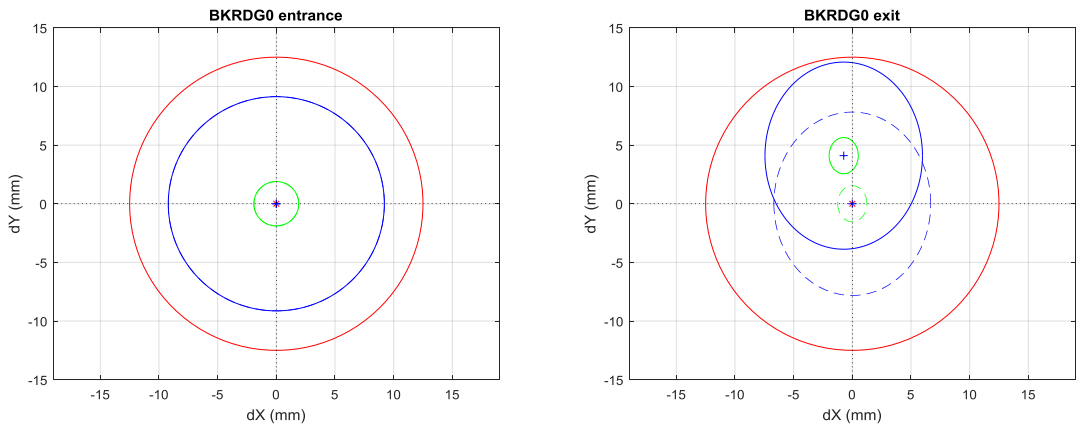

Figure 5: A cross-section of the 1-deg rolled **diagnostic kicker** chamber at its upstream end (left), and its downstream end (right). The plot shows the magnet bore with a 25-mm ID (red), the stay-clear of the unkicked beam (blue-dashed), and the stay-clear of the kicked beam (blue-solid). The ±6-sigma nominal beam sizes are also shown (green).

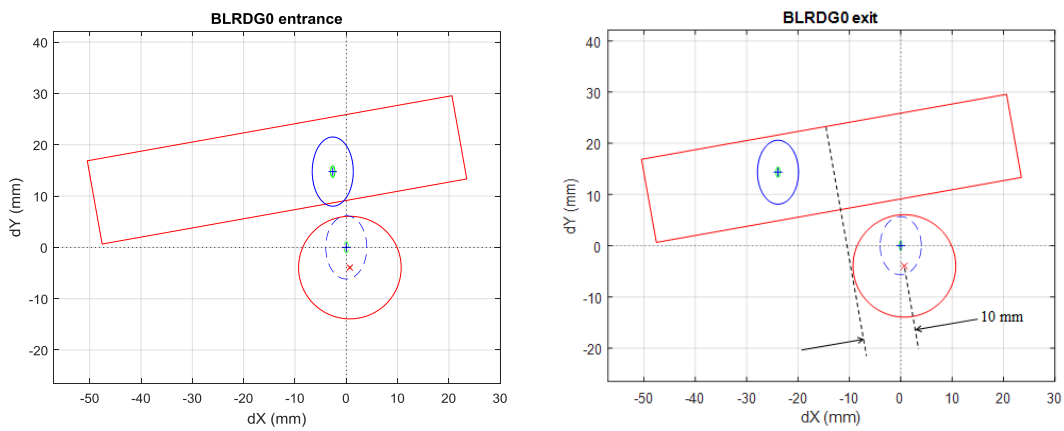

Figure 6: A cross-section (beam exits out of the paper) of 10-deg rolled **diagnostic septum** at its upstream end (left), and its downstream end (right). The plot shows the field-free cylindrical bore with a 20-mm ID (red-circle), the field-region rectangular aperture (red), the beam stay-clear of the unkicked beam (blue-dashed), and the stay-clear of the kicked beam (blue-solid). The ±6-sigma very small beam sizes are also shown (green). An intentional vertical offset of −4 mm (down) is added to the septum/chamber to safely enclose the stay-clear ellipses across the 3-mm iron separation bridge. The cylindrical aperture location is biased horizontally by 10 mm (to the right here) with respect to the center of the rectangular aperture, as shown in the right-side plot.

4 Spreader Kickers and Septa

The high-energy spreader kickers are described in Table 1 and Table 3, and the spreader septum magnet cross-section is shown in Figure 7, with a 20-mm ID field-free region and a 14.5-mm full vertical gap between the poles. The iron bridge separating the field-region from the field-free region is 3 mm thick at its narrowest.

For the spreader kickers, using the same TiN vacuum chamber coating, a 0.375-mm average vertical position along the kicker (for the kicked beam only), a 90-µm FWHM bunch length at 300 pC (or 30-µm at 100 pC), and the parameters listed in Table 3, the normalized wakefield kick for the kicked beam is $\Delta y'/\sigma_y' \approx 0.24$ for each spreader kicker, if no intentional alignment bias is added. This is small and equivalent to a < 3% relative emittance growth ($\Delta\varepsilon_y/\varepsilon_y \approx 0.5[\Delta y'/\sigma_y']^2$). The wakefield kick (without misalignment added) is the same for the SXR and the HXR kickers, with their nearly identical kicker and beam parameters.

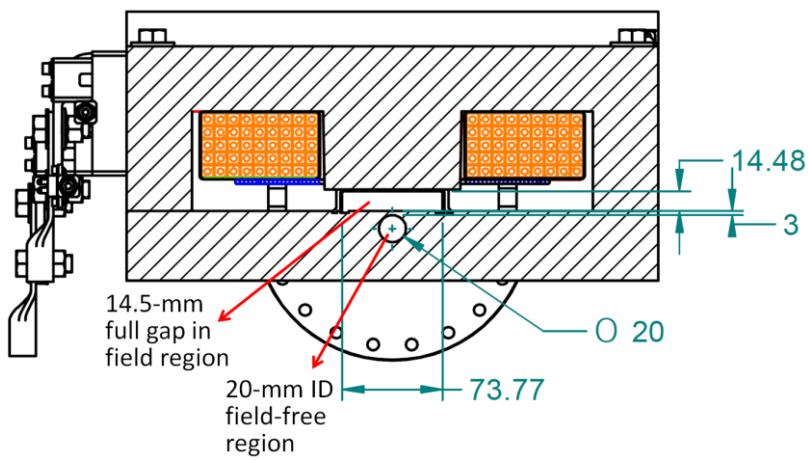

Figure 7: Cross-section of the **spreader septum magnet** with a 20-mm cylindrical ID in the field-free region, and a 14.5-mm full vertical gap in the rectangular field-region. The iron bridge separating the field-region from the field-free region is 3 mm thick at its narrowest. All dimensions in the figure are in mm.

To mitigate this wakefield effect in the spreader kickers, we choose to vertically bias (up) the HXR kicker/chamber by +0.2 mm (half of $\theta L/6$), and the SXR kicker/chamber by +0.4 mm ($\approx \theta L/6$), as shown in Figure 8. This redistributes the wakefields as listed below:

- The HXR beam, when its kicker fires, will see only the one wake-kick generated by the biased HXR kicker chamber producing a one-half ("+1/2") wake-kick of $\Delta y'/\sigma_y' \approx 0.24/2 = 0.12$ at the HXR kicker.
- With HXR kicker "*OFF*" (not triggered) the straight-ahead beam will see a wakefield kick generated by the vertically biased HXR kicker chamber, producing a minus-one-half ("–1/2") wake-kick of $\Delta y'/\sigma_y' \approx -0.24/2 = -0.12$ at the HXR kicker.
- So with HXR kicker off, this straight-ahead beam has two options. It can be deflected by the SXR kicker, or undeflected and directed straight to the BSY dump (see Figure 8).
- Since the SXR kicker has been vertically biased by $\theta L/6 \approx +0.4$ mm, no *additional* wakefield is generated for the SXR-kicked beam (its average trajectory is zero). The total wake for this beam is then just the one –0.12 kick which was generated back at the HXR kicker chamber (with kicker *OFF*).

- Finally, the beam which passes straight to the BSY dump will see the –0.12 kick, generated back at the HXR kicker chamber, and also the full ("–1") wake-kick (–0.24) generated by the vertically biased SXR kicker (with SXR kicker "*OFF*").

Note that the SXR beam sees both kicker chambers, while the HXR beam sees only one, but the wake effect on each beam is equal and opposite ($\Delta y'/\sigma_y' \approx \pm 0.12$), and also quite small. This is a compromise, **minimizing the wakes to 'half-strength' for each FEL beam**, but allowing a full wake-kick, plus an additional one-half wake after 100-deg of phase advance, $\Delta\psi_y$, on the BSY dump beam, since the beam quality in the dump line matters much less.

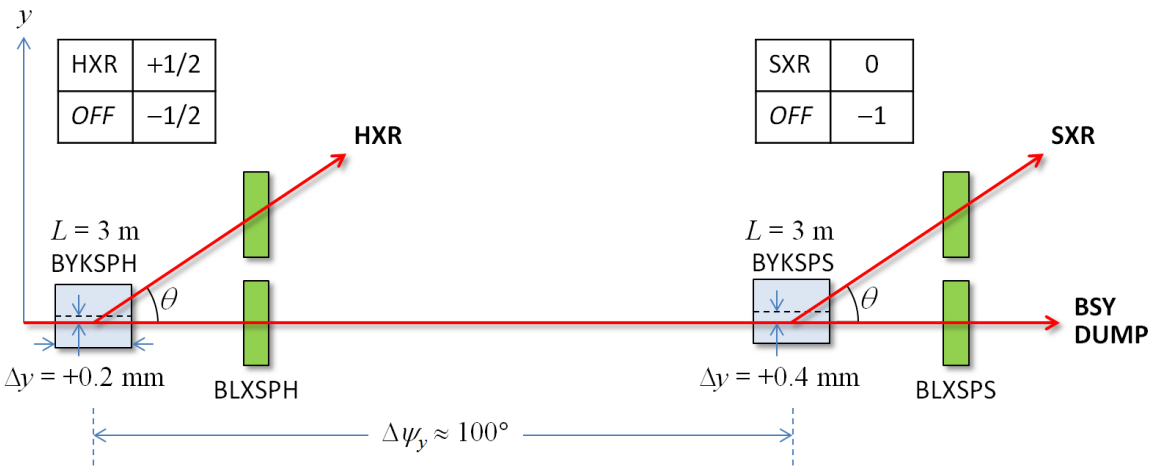

Figure 8: The spreader kickers with vertical alignment offsets, Δy, shown for each kicker. The HXR kicker/chamber is biased vertically (up) by +0.2 mm, while the SXR is biased (up) by +0.4 mm. The resulting wakes generate <1% emittance growth for each line. The septum magnet field-free and field-regions are represented by green blocks.

The HXR spreader kicker cross-section is shown in Figure 9 and shows the magnet vacuum chamber, the beam stay-clear, and the ±6-sigma beam sizes, shown before and after the kicker.

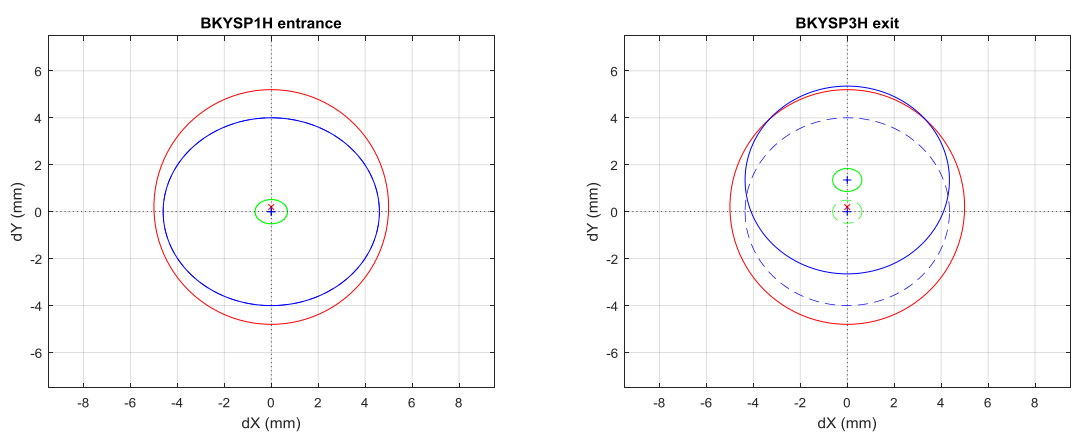

Figure 9: A cross-section of the **HXR kicker** chamber at its upstream end (left), and at its downstream end (right). The plot shows the bore with a 10-mm ID (red), the stay-clear of the unkicked beam (blue-dashed), and the stay-clear of the kicked beam (blue-solid). The ±6-sigma beam sizes are also shown (green). The HXR kicker/chamber is biased upward by +0.2 mm, as seen in the vertical separation of the blue "+" and the red "×".

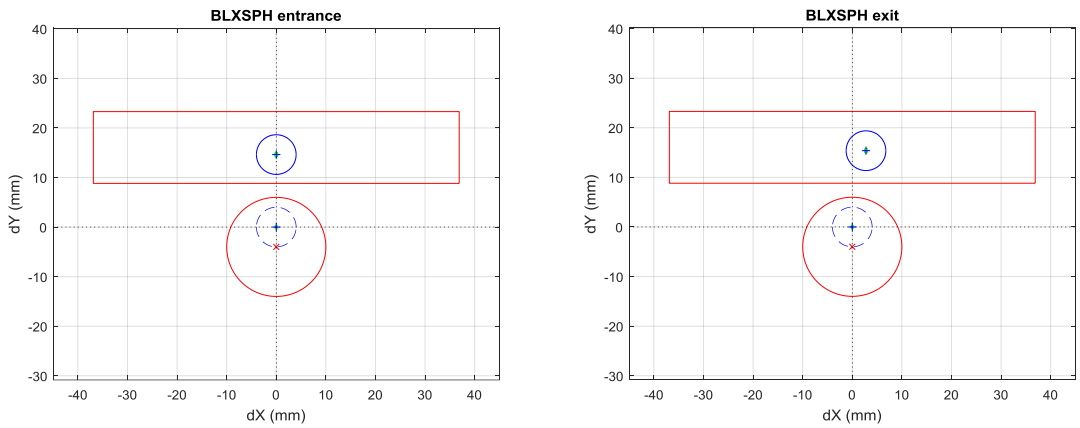

Figure 10: A cross-section (beam out of paper) of **HXR septum** magnet/chamber at its upstream end (left), and its downstream end (right). The plot shows the field-free magnet bore with a 20-mm ID (red-circle), the field-region aperture (red-rectangle), the stay-clear of the unkicked beam (blue-dashed), and the stay-clear of the kicked beam (blue-solid). The ±6-sigma beam sizes are also shown (green). An intentional vertical offset of –4 mm (down) is added to the magnet/chamber alignment to safely enclose the stay-clear ellipses. This is seen in the vertical separation of the lower blue "+" and red "×".

The SXR spreader kicker cross-section is shown in Figure 11 and shows the magnet vacuum chamber, the beam stay-clear, and the ±6-sigma beam sizes.

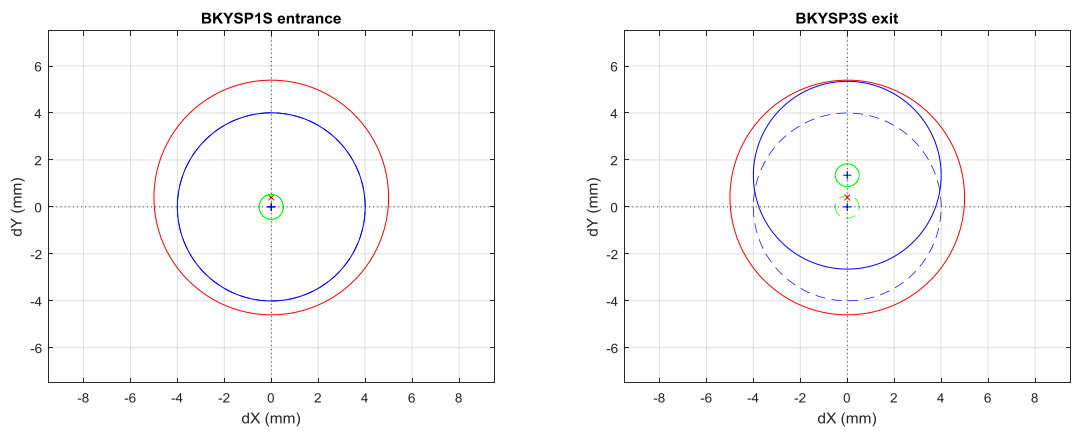

Figure 11: A cross-section (beam out of paper) of the **SXR spreader kicker** chamber at its upstream end (left), and its downstream end (right). The plot shows the bore with a 10-mm ID (red), the stay-clear of the unkicked beam (blue-dashed), and the stay-clear of the kicked beam (blue-solid). The ±6-sigma beam sizes are also shown (green). The SXR kicker/chamber is biased upward by +0.4 mm (up), as seen in the vertical separation of the blue "+" and red "×".

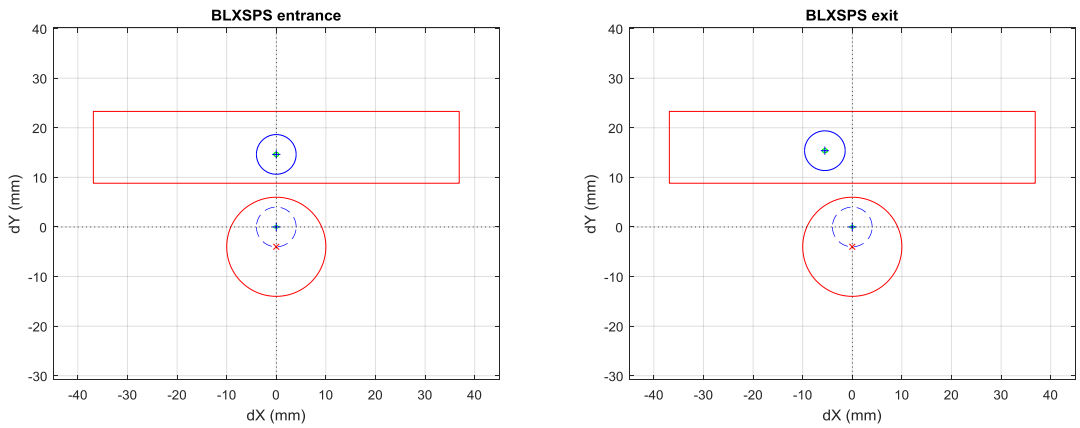

Figure 12: A cross-section (beam out of paper) of the **SXR septum** chamber at its upstream end (left), and at its downstream end (right). The plot shows the field-free magnet bore with a 20-mm ID (red-circle), the field-region aperture (red-rectangle), the stay-clear of the unkicked beam (blue-dashed), and the stay-clear of the kicked beam (blue-solid). The ±6-sigma beam sizes are also shown (green). An intentional vertical offset of –4 mm (down) is added to the magnet/chamber alignment to safely enclose the stay-clear ellipses. This is seen in the vertical separation of the lower blue "+" and red "×".

The septum magnets generate even smaller wakefields since these are DC magnets and do not require TiN-coated chambers. This allows stainless-steel ($\rho \approx 70$ μOhm-cm), and/or Nickel-Boron ($\rho \approx$ 10-90 μOhm-cm), which are less resistive than TiN. In addition, the septum magnets are shorter and with larger bores, but vertically offset, as described in the Figure **13** caption. The peak wakefields for the two spreader septum magnets are small ($\Delta y'/\sigma_y' < 0.04$), and summarized in Figure **13**, including wakes of the "field-region" (both rectangular chambers) and "field-free" region (cylindrical chamber). The SXR-field-free wake is a bit larger, but not shown since that beam goes to the BSY dump.

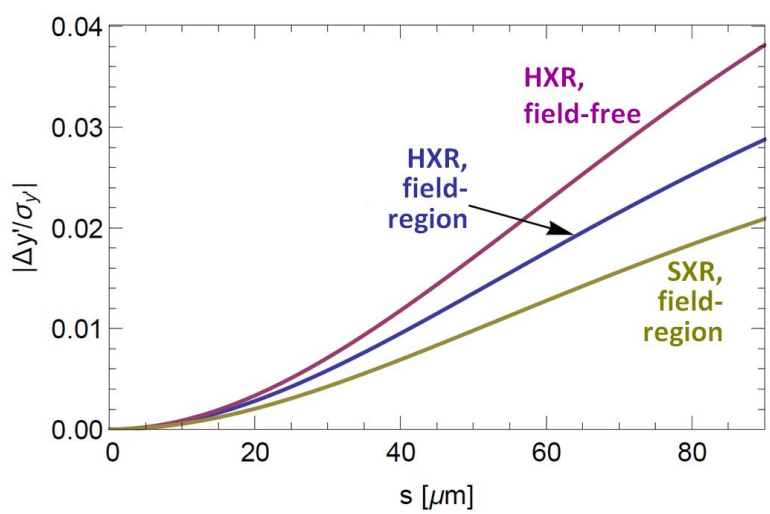

Figure 13: Transverse normalized wake ($\rho \approx 70$ μOhm-cm) for both **spreader septum magnets** evaluated along the bunch length coordinate, *s*, with vertical magnet offsets of 4 mm (HXR field-free) and ~1.25 mm (HXR & SXR field-regions). The beam distribution is uniform with 90-μm FWHM bunch length at 300 pC (or 30-μm at 100 pC). The SXR field-free wake is a bit larger, but not shown since that beam goes to the BSY dump.

Finally, the short diagnostic septum (see Table 2) is also offset by 4 mm (see Figure 6), but with a stainless-steel chamber it generates even less wake in the field-free region ($\Delta y'/\sigma_y' <$ 0.004). The wake of its field-region is smaller yet, due to a smaller beam offset (< 2 mm).

5 Summary

The transverse wakefield of the TiN-coated kicker vacuum chambers are minimized to an inconsequential level, and the beam stay-clear is maximized if we add small misalignments to the kicker and septum magnets in the LCLS-II. These misalignment requirements are summarized in Table 4. A positive vertical magnet/chamber offset in the tables implies that the magnet and vacuum chamber should be misaligned by this amount in the "up" direction. Note that these offsets especially apply to the vacuum chamber within the magnets, since the wakefield is generated by the interaction of the beam with the conducting vacuum chamber. Note that no horizontal offsets are needed, since the only relevant case (the diagnostic kicker) is already compensated in its design by displacing the cylindrical field-free aperture horizontally by 10 mm with respect to the center of the magnetic poles (see Figure 6, right-side plot). And finally, there are no significant *horizontal* wakefields, since the beam is always reasonably well centered horizontally in the kicker chambers and septum field-free regions, and the large width of the field-region rectangular apertures diminish the horizontal wake in each septum magnet.

Table 4: Required misalignments of **kicker** and **septa magnets**, with their chambers. In each case the vacuum chamber is assumed to be an integral part of the magnet. A positive Δy value here implies that the magnet/chamber needs to be displaced in the up direction with respect to the local beam axis. No horizontal magnet alignment offsets are needed.

Magnet	Parameter	symbol	DIAG0	HXR	SXR	units
Kicker	Vertical offset	Δy	0	+0.2	+0.4	mm
	Horizontal offset	Δx	0	0	0	mm
Septum	Vertical offset	Δy_s	–4.0	–4.0	–4.0	mm
	Horizontal offset	Δx_s	0	0	0	mm